Romanian Reports in Physics, Vol. 64, No. 4, P. 1032–1045, 2012

BIOPHYSISCS

NON-INVASIVE METHODS APPLIED FOR COMPLEX SIGNALS

R.R. NIGMATULLIN[1], C.M. IONESCU[2], S.I. OSOKIN[1], D. BALEANU[3], V.A. TOBOEV[4]

[1] Kazan Federal University, International Laboratory of Information Systems and Fractal Signal Processing, Institute of Physics, Kremlevskaya str. 18, Kazan, (Volga Region) Russian Federation
E-mail: renigmat@gmail.com
[2] Ghent University, Department of Electrical Energy, Systems and Automation, Technologiepark 913, 9052 Gent-Zwijnaarde, Belgium
[3] Cankaya University, Faculty of Art and Sciences, Department of Mathematics and Computer Sciences, Balgat 06530, Ankara, Turkey and Institute of Space Sciences, Magurele-Bucharest, Romania
[4] Chuvash State University, Department of Mathematics, 428015, Moskovskiy pr., 15, Cheboksary, Russia

Received February 16, 2012

Abstract. This paper presents the application of a novel algorithm on virtually generated data from patients during anesthesia. Realistic artefacts are simulated in order to validate the usefulness of the proposed methods in separating the signal components: biological trend and artefacts. The results show that the proposed new algorithm can be successfully employed on biological signals to dynamically extract information and distil useful parameters for clinical evaluation.

Key words: non-invasive methods, complex systems, anesthesia.

1. INTRODUCTION

Biological systems are nonlinear in nature and their corresponding measured signals are difficult to process in order to extract information, due to the presence of artifacts. Apart from these, biological signals have time-variant dynamics and nonlinear trends in their values. In medical applications, the intrinsic complexity of these signals pose challenges for filtering techniques and extraction of useful information for the clinicians.

An example of such challenging application is that of controlling the depth of anesthesia (DOA). Typically, there are three components defining the depth of anesthesia: hypnosis, analgesia and muscle relaxation. For measuring the hypnotic component of anaesthesia, various indexes are present, mostly computerized from

the spontaneous or evoked electroencephalogram (EEG) [1]. The bispectral index (BIS) is a single composite measure derived from the spontaneous EEG and has been proven to have a high sensitivity and specificity to measure anaesthetic drug effect [2]. BIS is now recognized as one of the reference measures of DOA for closed loop control purposes [3, 4]. In contrast to cerebral drug effect produced by hypnotics, an accurate measure for analgesia is still lacking. However, when BIS is known, a suitable interaction model between hypnotics and analgesics might be helpful to simultaneously control both components of DOA. Another important measure in systems controlling DOA is the electromiogram (EMG), an index which measures the degree of muscle relaxation. This index is important in surgery as well and in critically ill patients. However, this index is also corrupted by artefacts (eye movement, leg movement, shivering, etc). It is therefore important to provide a good separation between the actual EMG information on the patient and the artefacts.

This paper presents the application of a novel signal algorithm on virtually generated data from patients during anaesthesia. Realistic artefacts are simulated in order to validate the usefulness of the proposed methods in separating the signal components: biological trend and artefacts.

The paper is organized as follows: description of the patient model and simulated parameters is given in section two, followed by the description of the signal algorithm, filtering and modelling techniques in section three. The results are presented in the fourth section and a conclusion section summarizes the main outcome of this study.

2. PATIENT MODELING AND DATA GENERATION

Propofol is a hypnotic agent, for which the pharmacologic properties have been well described and studied in different kind of patients [1, 2, 5, 6]. Given its beneficial pharmacological profile, Propofol is used as one of the drugs of choice for both induction and maintenance of the hypnotic component of anesthesia and intensive care sedation. This drug is the input of the model and the output is the Bispectral Index (BIS), a signal derived from the electroencephalogram (EEG). Using EEG, several derived, computerized parameters like the BIS have been tested and validated as a promising measure of the hypnotic component of anesthesia 4]. BIS combines several features extracted from EEG including higher order spectra of the signal which can reveal phase coupling of single waveforms. Multivariate statistics were used to combine the different features into a single indicator value [2]. BIS values lie in the range of 0–100; whereas 90–100 range represents fully awake patients; 60–70 range and 40–60 range indicate light and moderate hypnotic state, respectively. For the induction phase of DOA, a BIS value of 50 is considered suitable.

In Fig. 1 the pharmacokinetic (PK) – pharmacodynamic (PD) blocks denote compartmental models.

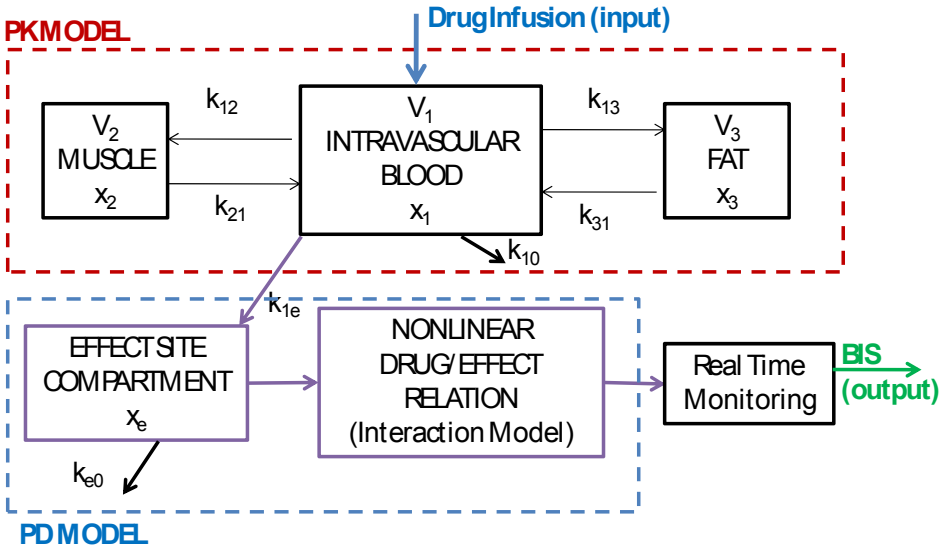

Fig. 1 – Compartmental model of the patient, where PK denotes the pharmacokinetic model and PD denotes the pharmacodynamic model.

Compartmental models are used to represent the distribution of drugs in the body, i.e. mass balance. They rely on a conservation principle applied to the exchange of chemicals among coupled macroscopic systems called compartments (central compartment, fast and slow equilibrating peripheral compartments). In each compartment the drug concentration is assumed to be uniform, as in a perfect and instantaneous mixing. The transport rate that leaves the compartment is assumed to be proportional to the drug concentration.

The PK-PD models are represented by the following equations (5–9):

$$\begin{aligned}
\dot{x}_1(t) &= -\left[k_{10} + k_{12} + k_{13}\right] \cdot x_1(t) + k_{21} \cdot x_2(t) + k_{31} \cdot x_3(t) + u(t), \\
\dot{x}_2(t) &= k_{12} \cdot x_1(t) - k_{21} \cdot x_2(t), \\
\dot{x}_3(t) &= k_{13} \cdot x_1(t) - k_{31} \cdot x_3(t), \\
\dot{x}_e(t) &= -k_{e0} \cdot x_e(t) + k_{1e} \cdot \frac{x_1(t)}{V_1},
\end{aligned} \tag{1}$$

where x_1 [mg] denotes the amount of drug in the central compartment. The blood concentration is expressed by x_1 / V_1. The peripheral compartments 2 and 3 model the drug exchange of the blood with well and poorly diffused body tissues. The masses of drug in fast and slow equilibrating peripheral compartments are denoted

by x_2 and x_3, respectively. The parameters k_{ji}, for $i \neq j$, denote the drug transfer frequency from the j^{th} to the i^{th} compartment and $u(t)$ [mg/s] is the infusion rate of the anesthetic drug into the central compartment. The parameters k_{ij} of the PK models depend on age, weight, height and gender and can be calculated for Propofol:

$$V_1 = 4.27 \ \ [l]$$
$$V_2 = 18.9 - 0.391 \cdot (age - 53) \ \ [l]$$
$$V_3 = 2.38 \ \ [l]$$
$$C_{l1} = 1.89 + 0.0456(weight - 77) - 0.0681(lbm - 59) +$$
$$+0.0264(height - 177) \ \ [1/\min]$$
$$C_{l2} = 1.29 - 0.024(age - 53) \ \ [1/\min]$$
$$C_{l3} = 0.836 \ \ [1/\min]$$
$$k_{10} = \frac{C_{l1}}{V_1} \ \ [\min -1], \quad k_{12} = \frac{C_{l2}}{V_1} \ \ [\min -1], \quad k_{13} = \frac{C_{l3}}{V_1} [\min^{-1}],$$
$$k_{21} = \frac{C_{l2}}{V_2} \ \ [\min^{-1}], \quad k_{31} = \frac{C_{l3}}{V_3} [\min^{-1}],$$

where C_{l1} is the rate at which the drug is cleared from the body, and C_{l2} and C_{l3} are the rates at which the drug is removed from the central compartment to the other two compartments by distribution. The lean body mass (lbm) for men and women have the following expressions: $\text{lbm} = 1.1 \cdot weight - 128 \cdot \frac{weight^2}{height^2}$ and $\text{lbm} = 1.07 \cdot weight - 148 \cdot \frac{weight^2}{height^2}$, respectively.

An additional hypothetical effect compartment was proposed to represent the lag between drug plasma concentration and drug response. The concentration of drug in this compartment is represented by x_e. The effect compartment receives drug from the central compartment by a first-order process and it is regarded as a virtual additional compartment. Therefore, the drug transfer frequency from the central compartment to the effect site-compartment is equal to the frequency of drug removal from the effect-site compartment: $k_{e0} = k_{1e} = 0.456 \min^{-1}$. Knowing k_{e0}, the apparent concentration in the effect compartment can be calculated since k_{e0} will precisely characterize the temporal effects of equilibration between the

plasma concentration and the corresponding drug effect. Consequently, the equation is often used as:

$$\dot{C}_e(t) = k_{e0} \cdot (C_e(t) - C_p(t)), \tag{2}$$

with C_e called the *effect-site compartment concentration*. The BIS variable can be related to the drug effect concentration C_e by the empirical static but time varying nonlinear relationship, called also the *Hill curve:*

$$BIS(t) = E_0 - E_{\max} \cdot \frac{C_e(t)^{\gamma}}{C_e(t)^{\gamma} + C_{50}^{\gamma}}, \tag{3}$$

where E_0 denotes the baseline (awake state – without drug) value, which, by convention, is typically assigned a value of 100, $E_{\max}$ denotes the maximum effect achieved by the drug infusion, C_{50} is the drug concentration at half maximal effect and represents the patient sensitivity to the drug, and γ determines the steepness of the curve.

The data for this study has been derived from a set of 3 virtually generated realistic patients, with the biometric values given in Table 1.

Table 1

Biometric values of the patients selected for this study

Patient	Age [years]	Length [cm]	Weight [kg]	Gender	Γ	C50
1	53	186	114	M	1.99	6.7
7	71	172	83	M	2.76	4.6
17	72	162	87	M	2.30	3.9

3. DESCRIPTION OF THE TREATMENT PROCEDURE

Initial data are treated by the following way. Firstly, we apply the procedure of the optimal linear smoothing (POLS). The POLS is described in papers [10–14]. This procedure helps to find the optimal and smoothed trend (the so-called pseudo-fitting function) and separate it from the relative fluctuations. Minimizing the value of the relative error on the plot "relative error with respect to the value of the smoothing window" in the vicinity of the first local minima, one can obtain the pseudo-fitting function without information related to the mathematical model used. Besides this important peculiarity the new method enables “to read” the remaining detrended noise and express the desired distribution in terms of the fitting parameters corresponding to the envelope of the sequence of the ranged

amplitudes (SRA). Let us suppose that the random sequence considered contains large-scale fluctuations (trend) and high-frequency fluctuations, which are usually determined as a "noise". In order to separate those from each other we apply the procedure of the optimal linear smoothing (POLS) based on the Gaussian kernel. This procedure is defined as

$$\tilde{y} = Gsm\left(x,\ y,\ w\right) = \frac{\sum_{j=1}^{N} K\left(\frac{x_i - x_j}{w}\right) y_j}{\sum_{j=1}^{N} K\left(\frac{x_i - x_j}{w}\right)}, \quad K\left(t\right) = \exp\left(-\frac{t^2}{2}\right). \tag{4}$$

Here the function $K(t)$ defines the Gaussian kernel, the value w defines the current width of the smoothing window. The set y_j (j = 1, 2, …, N) defines the initial noisy sequence. In spite of the fact that there are many smoothing functions imbedded in many mathematical programs this chosen function has two important features: (a) the transformed smoothed function in (4) is obtained in the result of linear transformation and does not have uncontrollable error; (b) the value of the smoothing window (w) is adjustable (fitting) parameter and accept any positive value. This function in a certain sense can be considered as a pseudo-fitting function, which is not associated directly with a specific model describing the desired process. The value of the optimal window w_{opt} is chosen from the conditions:

$$\begin{aligned} &\Delta n_j = y_j - Gsm\left(x,\ \tilde{y},\ w\right), \\ &\tilde{y}_{w'} = Gsm\left(x,\ \tilde{y}_w,\ w'\right),\ w' < w, \\ &\min\left(RelErr\right) = \left[\frac{StDev\left(\left|y_{w'} - y_w\right|\right)}{Mean\left(y_w\right)}\right] \cdot 100\ \ \%. \end{aligned} \tag{5}$$

This procedure automatically decreases the value of the initial fluctuations by means of iteration procedure and helps to find the optimal smoothing window value w_{opt} minimizing the value of the relative error, defined as RelErr(w), in the vicinity of the first local minimum. Here it is necessary to stress the following fact. The behavior of the function RelErr(w) realized for many original and mimic random sequences with hidden (uncertain) trend has some specific features. This function has at least three minimal points or even more. "Zero" minimal point coincides with the *global* minimum when the value of w is very close to the given discrete step ($h = \Delta x$). The last minimal point coincides with the large values of w, corresponding to mean value of the random sequence analyzed. The first local minimum can appear after the global (zero) minimum. In many model calculations realized with random sequences having clearly expressed or hidden trends this

optimal value w_{opt} does exist that helps to find the optimal smoothed curve (trend) describing the large-scale fluctuations. The desired trend minimizing the value of the relative error is described by expression

$$\tilde{y} = Gsm\left(x,\ y,\ \tilde{w}\right),\ \tilde{w} \equiv w_{opt}\,. \tag{6}$$

After calculation of the optimal trend it becomes possible to separate initial random sequence on two parts: (a) the optimal trend expressed by relationship (6) and (b) detrended sequence representing the values of the *relative fluctuations*, which is expressed as

$$srf = y - \tilde{y}\,. \tag{7}$$

Here *srf* defines the de-trended sequence of the relative fluctuations. This method helps to divide initial noise on two parts: trend (defined here as the pseudo-fitting function) and relative fluctuations.

In addition to the previous procedure, we apply the POLS to all data which were obtained in the result of the numerical integration of the previous data. Mathematically it can be expressed by means of the following iteration algorithm

$$\begin{aligned} &Jy_j = Jy_{j-1} + \frac{1}{2}\left(x_j - x_{j-1}\right)\left(\Delta y_j + \Delta y_{j-1}\right), \quad Jy_0 = 0, \quad j = 1,2,...,N \\ &\Delta y_j = y_j - \frac{1}{N}\sum_{j=1}^{N} y_j. \end{aligned} \tag{8}$$

This integral transformation (calculated by the trapezoid method) helps to see clearly the trend (which can be hidden in initial data) and facilitate the application of the POLS to the corresponding integral curves. It means that in expression (4) we should replace $y_j \to Jy_j$. Then one can find the smoothed trends applying the differentiation operation to the trends found for integral curves

$$D\left(J\tilde{y}_j\right) = \frac{J\tilde{y}_j - J\tilde{y}_{j-1}}{x_j - x_{j-1}}. \tag{9}$$

This idea was applied in paper [15] when initial data were strongly deviated and trend was hidden inside initial data.

4. RESULTS

Figures 2a and b clearly show the idea of POLS.

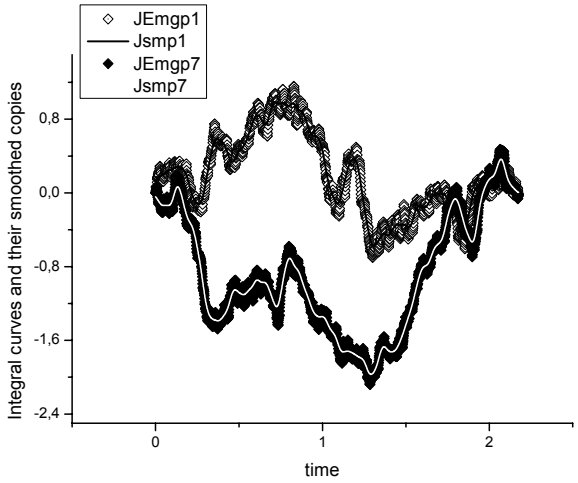

Fig. 2a – The integrated curves obtained for EMG data (patients 1–upper curve and patient 7 – lower curve). The optimal trends are shown by solid lines. The data for the third patient is not shown in order to provide a clear view.

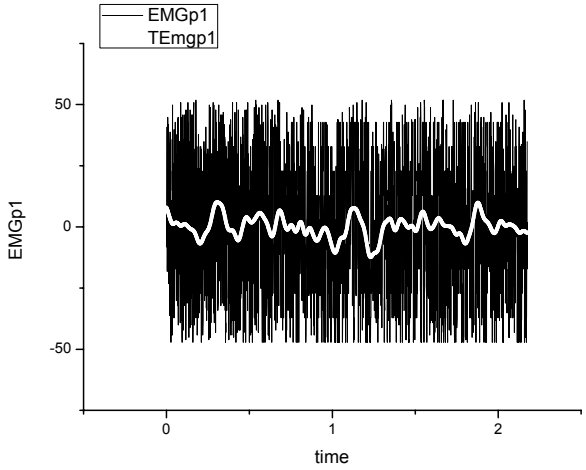

Fig. 2b – The initial EMG data (patient 1) shown by black solid lines.
The optimal trend is shown by bold white line.

Figure 2a demonstrates the integral curve found for EMG data (muscular activity – patient 1 and 7). The smoothed curves are shown by solid line. After differentiation of the smoothed integral curve (calculated with the help of expression (9)) we obtain the desired smoothed curve for initial data where the calculation of the optimal trends by conventional methods is hopeless situation. For patient 1 it is shown on Fig. 2b. Figure 3a demonstrates all initial trends found for EMG data (recorded for three patients).

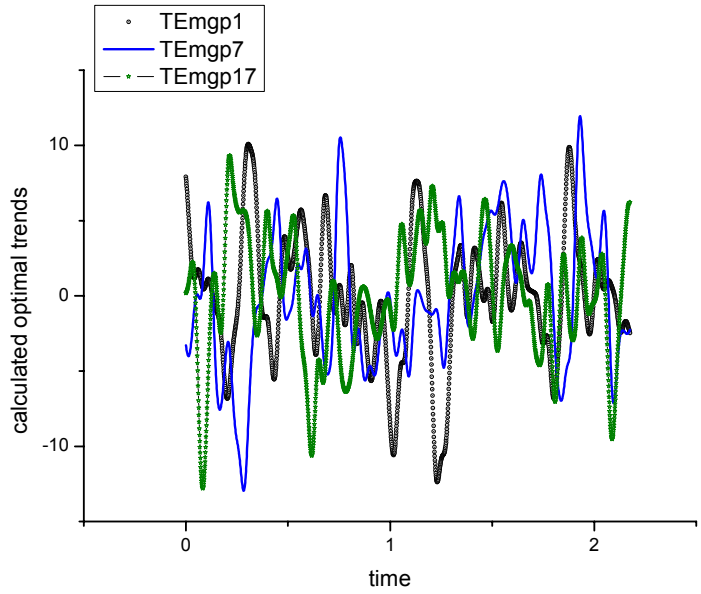

Fig. 3a – The optimal trends calculated for EMG data. These trends have a strong oscillatory character and are difficult for analysis. It is much easier to analyze their integral curves. These are shown below in Fig. 3b.

Similarly, one can find the desired trends for BIS (brain activity) data. The optimal trends for the integrated curves are shown on Fig. 3b.

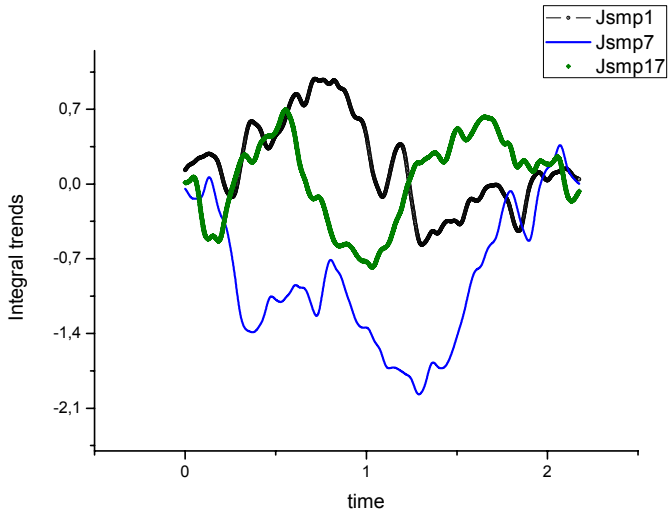

Fig. 3b – The optimal trends obtained for integral curves presenting the EMG data. As one can notice from comparison with Fig. 3a, the integration suppresses the high frequency fluctuations and facilitates the analysis of initial data.

Consequently, Fig. 4a depicts the trends for initial BIS data and the corresponding integrated trends are collected on Fig. 4b.

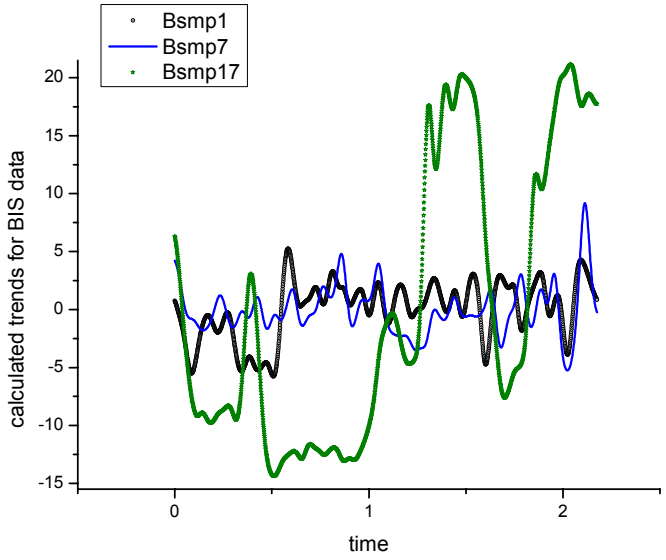

Fig. 4a – The optimal trends for BIS data found at the same conditions (the optimal value of the smoothing window $w \approx 0.03$).

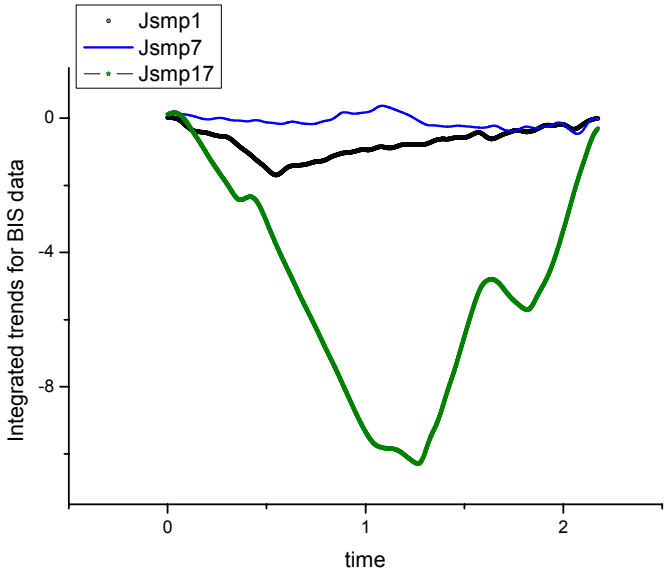

Fig. 4b – The integration procedure suppresses the high-frequency oscillations for BIS data and in many cases facilitates the analysis of complex data. The black color is associated with patient 1, the blue one to p. 7 and green color to p. 17, correspondingly.

Again we notice that the high-frequency fluctuations are suppressed leaving the low-frequency modes for further analysis.

The remnant functions contain also some information expressed in terms of the fitting parameters of the corresponding distribution. The remnant function in general case is determined as

$$R(t) = Nin(t) - Trend(t)\,, \tag{10}$$

where $Nin(t)$ determines the initial random sequence and $Trend(t)$ determines the trend found with the help of the POLS. After calculation of $R(t)$ it is necessary to form the sequence of the ranged amplitudes (SRA). This sequence $Sr(t)$ satisfies the condition: $Sr_0 > Sr_1 > \ldots > Sr_N$. As it has been shown earlier [14b] the found SRA being integrated in the same temporal interval forms the bell-like curve and in many cases can be fitted to the beta-distribution function. So, one can write approximately

$$J(t) = \int_{t_0}^{t} Sr(t)\mathrm{d}t \simeq A\left(t - t_0\right)^{\alpha}\left(t_N - t\right)^{\beta} + B\,. \tag{11}$$

So, for many cases any strongly-correlated noise can be read in terms of the fitting parameters (A, B, α, β) corresponding to the desired beta-distribution. For EMG data the basic steps of this transformation are shown on Figs. 4a,b. The fit of the bell-like curves for patient 1 is shown on Fig. 5.

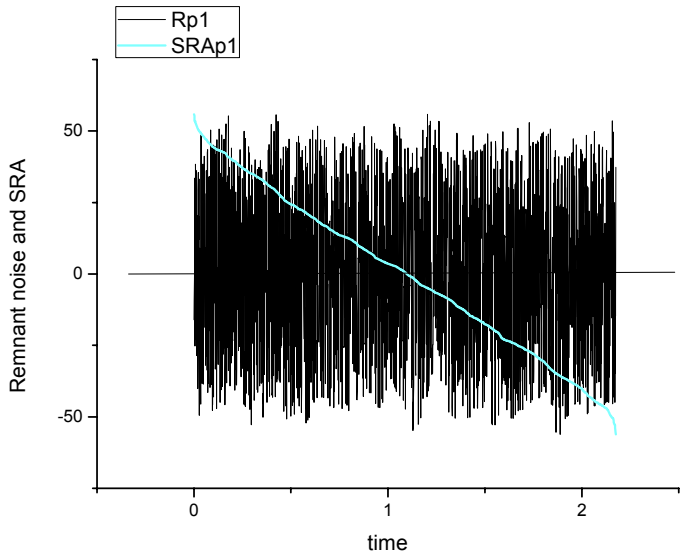

Fig. 5 – Remnant noise obtained for EMG data (patient 1). The SRA is shown by blue line.

The fit of the remnant noise to the beta-distribution function is presented in Fig. 6.

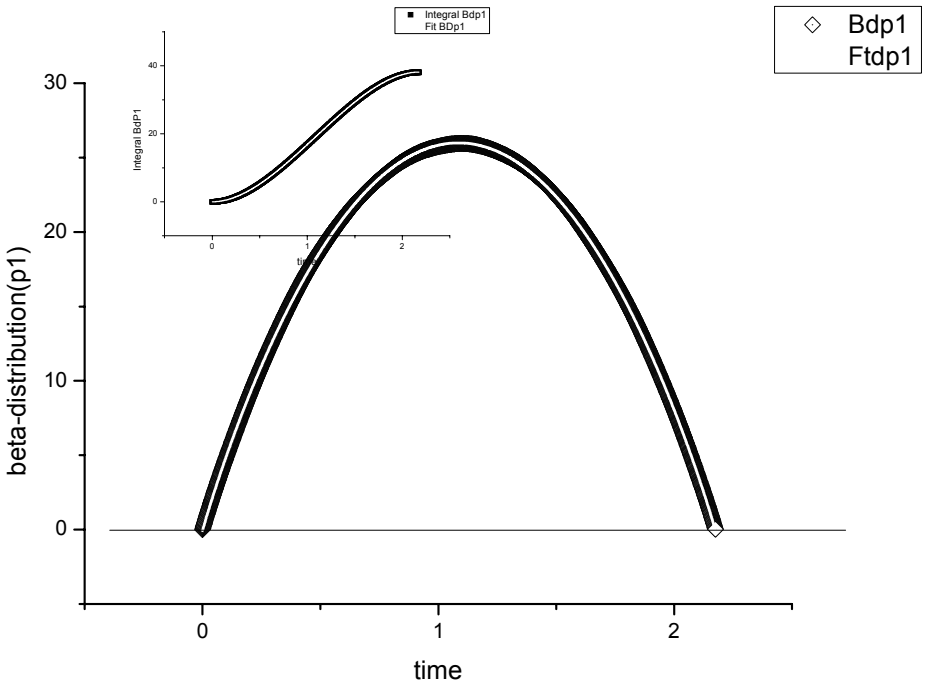

Fig. 6 – The ECs method allows to fit simultaneously the integral taken from this distribution. This fit is shown on the small figure above. Other similar fits corresponding to other remnant noises look similar and are not shown. We do not show the fitting parameters because the systematic analysis of these quantitative values in this paper is absent.

All fitting parameters corresponding to Eqn. (2) are collected in Table 1.

From Fig. 2b it is possible to observe that the trend of the EMG is very well separated and ready for clinical use. In DOA, this information is very useful in a feedback closed loop control context, providing information upon the state of the muscle relaxation in the patient. If this trend is above a certain imposed threshold, the anesthesiologist can decide to increase the target infusion for the corresponding drug. Similarly, Fig. 3b shows the impact of the integration, allowing a clear separation between the three simulated patient data. Typically, the inter-patient variability is very difficult to classify by evaluating the result from Fig. 3a only. As such, the EMG trends overlap and the sensitivity of the patient to the drug is not estimated correctly. The solution to this problem is then clearly shown in Fig. 3b.

Similarly, the BIS signal from Fig. 4a overlap for the three types of patient sensitivity to the propofol drug (given mainly by the change in the γ parameter from Table 1). It is observed that patient 17 has high oscillations in the BIS value, indicating strong artifact presence and a poor sedation level. Again, the effect of integration is more pronounced, as depicted in Fig. 4b, showing the clear separation of the three cases. This information is then more useful to the automatic control of

DOA, since it provides the slope of changes in BIS signal affected by the artifact presence. In this context, the controller will react much faster and much more accurate based on the information from Fig. 4b than the information from Fig. 4a, by setting the suitable drug infusion rate into the patient.

5. CONCLUSIONS

So, in this paper we demonstrated preliminary possibilities of new methods that can be defined as non-invasive methods of the reduced analysis of data (NIMRAD). In the next publications related to analysis of biological signals we show *how* to apply the NAFASS approach [16] for finding the informative-frequency band of frequencies (amplitude frequency response) and separate the non-stationary parts of the complex signal from quasi-stationary parts. This separation is based on the statistics of the fractional moments [11,16,17] that helps to find more accurately the range of correlations on the whole range of moments (in practice the total range of moments is located between the values $[e^{-15}, e^{15}]$ where e is the Euler number.

Acknowledgements. Two authors (RRN, SIO) express their sincere acknowledgements for the grant (number of grant 1.84.11) of the Ministry of Higher Education and Science of the Russian Federation for its financial support. The last author (VAT) wants to express his satisfaction for the possibility to have collaboration with the recently created on the base of the Kazan (Volga region) Federal University "International Laboratory of Information Systems and Fractal Signal Processing".

Clara Ionescu would like to acknowledge the post-doctoral financial support from Flanders Research Centre (FWO) Belgium.

REFERENCES

1. T. De Smet, MM. Struys, MM. Neckbroek, K. Van den Hauwe, S. Bonte, E.P. Mortier, *The accuracy and clinical feasibility of a new bayesian-based closed-loop control system for propofol administration using the bispectral index as a controlled variable*, Anesth. Analg., **107**, 1200–10 (2008).
2. M. Struys, H. Vereecke, A. Moerman, EW. Jensen, D. Verhaeghen, N. De Neve, FJ. Dumortier, EP. Mortier, *Ability of the bispectral index, autoregressive modelling with exogenous input-derived auditory evoked potentials, and predicted Propofol concentrations to measure patient responsiveness during anesthesia with Propofol and Remifentanil*, Anesthesiology, **99**, 802–12 (2003).
3. C. Ionescu, R. De Keyser, B.C. Torrico, T. De Smet, M. Struys, J.E. Normey-Rico, *Robust Predictive Control Strategy Applied for Propofol Dosing using BIS as a Controlled Variable during Anesthesia*, IEEE Transactions on Biomedical Engineering, **55**, 2161–2170 (2008).
4. M. Struys, T. De Smet, L. Versichelen, *System and method for adaptive drug delivery*, US Patent 6605072, 2003.
5. T.W. Schnider, C.F. Minto, P.L. Gambus , C Andresen, DB Goodale , EJ Youngs, *The influence of method of administration and covariates on the pharmacokinetics of Propofol in adult volunteers*, in Anesthesiology, **88**, 1170–1182 (1998).

6. TW. Schnider, CF Minto, SL Shafer, PL Gambús, C Andresen, DB Goodale, EJ Youngs, *The influence of age on Propofol pharmacodynamics*, Anesthesiology, **90**, 1502–16 (1999).
7. B. Marsh, M. White, N. Morton, GN. Kenny, *Pharmacokinetic model driven infusion of Propofol in children*, British Journal of Anaesthesia, **67**, 41–8 (1991).
8. CF Minto, M White, N Morton, GN Kenny, *Pharmacokinetics and pharmacodynamics of reminfetanil. II Model application*, Anesthesiology, **86**, 24–33 (1997).
9. CF Minto, TW Schnider, TD Egan, E Youngs, HJ Lemmens, PL Gambús, V Billard, JF Hoke, KH Moore, DJ Hermann, KT Muir, JW Mandema, SL Shafer, *Influence of age and gender on the pharmacokinetics and pharmacodynamics of reminfetanil. I. Model development*, Anesthesiology, **86**, 10–23 (1997).
10. R.R. Nigmatullin, *Strongly Correlated Variables and Existence of the Universal Disctribution Function for Relative Fluctuations*, Physics of Wave Phenomena, **16,** *2*, 119–145 (2008).
11. Raoul R. Nigmatullin, Dumitru Baleanu, Erdal Dinc, and Ali Osman Solak, *Characterization of a benzoic acid modified glassy carbon electrodes expressed quantitatively by new statistical parameters*, Physica E, **41**, 609–614 (2009).
12. R.R. Nigmatullin, H. Nakanishi, Q. Miyata, D. Tahara, K. Fukao, *Application of new treatment methods for* "reading" *of the complex capacitance: a quantitative description of the aging phenomenon in polymer glasses*, Communications in Nonlinear Science and Numerical Simulation, **15**, *5*, 1286–1307 (2010).
13. R.R. Nigmatullin, T. Omay, D. Baleanu, *On fractional filtering versus conventional filtering in economics*, Communications in Nonlinear Science and Numerical Simulation, **15**, *4*, 979–986 (2010).
14. (a) R. R. Nigmatullin, *New Noninvasive Methods for* "Reading" *of Random Sequences and Their Applications in Nanotechnology*. *New Trends in Nanotechnology and Fractional Calculus Applications*, Ed. D. Baleanu, Z. B. Guvenc, J.A. Tenreiro Machado, Springer, 2010, pp. 43–56. See also: R.R. Nigmatullin, *Universal distribution function for the strongly-correlated fluctuations: general way for description of random sequences*, Communications in Nonlinear Science and Numerical Simulation, **15**, 637–647 (2010).
15. R.R. Nigmatullin, I.I. Popov, and D. Baleanu, *Predictions based on the cumulative curves: Basic principles and nontrivial example* Communications in Nonlinear Science and Numerical Simulation, **16**, 895–915 (2011).
16. R.R. Nigmatullin, S.I. Osokin and V.A. Toboev, *NAFASS: Discrete spectroscopy of random signals*, Chaos, Solitons and Fractals, **44**, 226–240 (2011).
17. R.R. Nigmatullin, *The statistics of the fractional moments: Is there any chance to read "quantitatively" any randomness*?, Journal of the Signal Processing, **86**, 2529–2547 (2006).